Cellulose nanowhisker aerogels

Lindy Heath and Wim Thielemans*

Received 23rd April 2010, Accepted 15th June 2010
First published as an Advance Article on the web 13th July 2010
DOI: 10.1039/c0gc00035c

Aerogels were prepared through the self-assembly of cellulose nanowhiskers in a benign manner. Preparation of these aerogels only requires sonication in water to form a hydrogel, solvent exchange with ethanol and supercritical CO_2 drying. Aerogels were prepared with varying cellulose nanowhisker content and characterised with X-ray diffraction, BET analysis and electron microscopy. Their density and porosity varied linearly with varying concentrations of cellulose nanowhiskers in the initial hydrogel and confirmed that gel shrinkage upon drying was limited to, on average, 6.5%. We achieved densities down to 78 mg cm^{-3} with high specific surface areas up to 605 m^2 g^{-1}. Mesopores displaying a bimodal size distributions with maxima centred around 4.3 and 15.5 nm accounted for 5–11% of total pore volume. Micropores accounted for less than 1% of total pore volume with the remaining fraction being macropores.

Introduction

Aerogels are non-periodic porous nanostructured materials which exhibit unusual properties, such as high porosity and surface area, low density, and low heat conductivity.[1] S. Kistler synthesized the first aerogels in the 1930s from a variety of materials such as silica, alumina, rubber and cellulose-derivatives.[2] He also introduced the methods for producing aerogels which is still actively used today. Initially, a wet gel (a hydrogel) is formed, which is solvent exchanged with a water-soluble alcohol to yield an alcogel. The alcogel is then dried under supercritical conditions to form the aerogel, a process in which the highly porous structure of the alcogel is retained.[3]

A wide variety of aerogels have been reported in the literature. They can be produced from silica, alumina, tin oxide, chromia and carbon, with silica the most widely used.[4] These aerogels typically display porosities up to 99%, bulk densities in the range 0.004–0.500 g cm^{-3}, and surface areas between 100 and 1000 m^2 g^{-1}.[4,5] The differences in structural characteristics are attributed to the various production methods and starting materials.[6] The unique properties associated with aerogels have lead to their use in a wide range of applications such as catalysts,[6] catalyst supports,[4] super-thermal and sound insulators,[4,7] electronics,[8] particle filters,[8] in space and particle research[7] and as a storage media for gases in fuel cells.[8] More recently, cellulose has gained interest as a source material for the production of aerogels due to its renewability and biodegradability.[8] Cellulose aerogels have proven particularly useful in applications where biocompatibility and biodegradability are needed, such as for medicinal, cosmetic and pharmaceutical applications, opening up the application fields of aerogels even more.[9] Several approaches exist, most of which use either cellulose derivatives or cellulose-dissolving solvents followed by a regeneration step.[10] In a different approach, Pääkko *et al.* recently reported a low surface area, flexible aerogel made from microfibrillated cellulose,[11] while Gawryla *et al.* reported on a clay/cellulose nanowhisker composite with a porous structure.[12] The latter however is rather a loose assembly of solid nanoparticles than an aerogel since a gelled network is not formed before drying. This results in relatively low surface area materials as has been shown previously using starch nanocrystals.[13] Mesoporous bacterial cellulose aerogels with an average density of 8.25 mg cm^{-3} and a specific surface area of 200 m^2 g^{-1} have also been reported recently.[14] These were formed by solvent exchanging and supercritical CO_2 drying of cellulose hydrogels produced directly by the gram-negative baterium *Gluconacetobacter xylinum* over 30 days.

Cellulose nanowhiskers are rigid rods with a rectangular cross section with dimensions between 3 and 20 nm and lengths ranging between 100 nm and several microns.[15,16] They are extracted from native cellulose through an acid hydrolysis procedure using a concentrated aqueous inorganic acid solution. Diffusion of hydronium ions into the amorphous cellulose regions is aided by free volume effects, resulting in a selective hydrolysis of these sections. The crystalline sections will hydrolyse after being released from the cellulose matrix into the acid, so that careful timing of the reaction allows one to recover individualised crystalline cellulose particles. These particles are highly crystalline nanosized rigid rods and can be assembled in membranes held together by strong hydrogen bonds formed upon drying.[17] Micrometre thin films displayed pores with pore sizes around 50 nm. Based on these results it can be conceived that at high concentration, cellulose nanowhiskers will form a three-dimensional hydrogen bonded network when dispersed using forces of the same order of magnitude or lower as hydrogen bonds. As the water cavitation energy is of the same order of magnitude as the energy of hydrogen bonds (4–50 kJ mol^{-1}),[18] it should be possible to form homogeneous cellulose nanowhisker hydrogels through low-power sonication.

Within the same idea, Tischer *et al.* used high power ultrasound treatment to reorganize microfibrillar bacterial cellulose

School of Chemistry and Process and Environmental Research Division-Faculty of Engineering, The University of Nottingham, University Park, Nottingham, NG7 2RD, UK. E-mail: wim.thielemans@nottingham.ac.uk

by inducing crystallisation of amorphous regions and fusion of neighboring cellulose crystallites.[18] The crystalline regions were said to be less affected than the amorphous regions as water penetration is reduced due to lower free volume in the crystalline regions. In the work presented in this manuscript, we use a low power ultrasound bath to disperse cellulose nanowhiskers in water at a concentration well above the percolation threshold, resulting in a hydrogen-bonded hydrogel. The ultrasound treatment does not alter or destroy the crystalline structure but it enables the formation of hydrogen bonds between the nanowhiskers (Fig. 1), resulting in a stable gelled hydrogen-bonded network in deionised water. Solvent exchange with ethanol resulted in an alcogel which was then dried using supercritical CO_2 ($scCO_2$) to form aerogels with high specific surface area and very low density. The formation of the aerogel from cellulose nanowhiskers is benign, using $scCO_2$, water and ethanol, to produce high surface area cellulose aerogels, improving on the use of dissolved molecular cellulose or cellulose derivatives as the structural component.

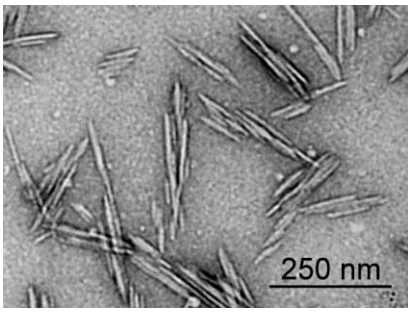

Fig. 1 Transmission electron micrograph of cellulose nanowhiskers derived from cotton.

Experimental

Cotton wool was supplied by Boots Ltd. and was used as received. Sulfuric acid (>95% purity) was supplied by Fischer Scientific and was used as a 64 wt% aqueous solution after dilution. Amberlite MB 6113 was supplied by Fluka. Carbon dioxide (purity 99.9%) was supplied by Cryoservice, and anhydrous ethanol was received from Sigma Aldrich and used as received. Deionised water was used in all experiments.

Cellulose nanowhiskers were obtained by the acid hydrolysis of cotton wool for 35 min at 45 °C in a 64 wt% aqueous H_2SO_4 solution under constant stirring. The cellulose nanocrystals were then washed with distilled water and centrifuged for 20 min at 10 000 rpm and 10 °C. The supernatant was discarded and the sedimented nanoparticles were redispersed in deionised water and recentrifuged. This was repeated a third time. Dialysis of the nanocrystals for 48 h against tap water was then used to remove any remaining free acid. Nanoparticles were redispersed by sonication using a Branson sonifier for 5 min, in three second pulses with two second intervals at an amplitude of 15% of maximum power while making sure the temperature did not breach 30 °C. Aggregates were removed by filtration over a No. 2 fritted filter. Amberlite NB 6113 was then added under agitation for one hour to the dispersion to protonate the surface of the cellulose nanocrystals and was subsequently removed by filtration. The suspension was redispersed using the sonifier for approximately two minutes. After the final sonication, the dispersion was plunged into liquid nitrogen to freeze before being attached to a Heto PowerDry LL3000 Freeze Dryer until it was completely dry. It has to be noted that the sulfuric acid employed is recovered in the first centrifugation step together with glucosidic breakdown products. While not investigated in this work, removal of the organic hydrolysis products enables recovery of the aqueous acid allowing recycling of the aqueous acid with the same purity after reconcentrating.

The freeze-dried cellulose nanowhiskers were used to produce aerogels in a three step method. A hydrogel was produced using varying concentrations of nanowhiskers by dispersion in 1 ml deionised water at 25 °C using a sonication bath (Sonomatic 375 Ultrasonic Cleaner, Agar Scientific). The sonication bath has a frequency of 40 kHz and a high frequency power output of 75 W. Sonication was performed in 15 min intervals until gelation. The gelation point was determined as the point in which the vial mould could be inverted without net movement of the gel. The hydrogel was then subjected to solvent exchange in an excess of anhydrous ethanol for four days at 25 °C, changing the ethanol every 24 h, to obtain an alcogel. This alcogel was subsequently dried under $scCO_2$† in a flow-through autoclave at a temperature of 40 °C and a pressure of 100 bar. The flow of carbon dioxide was kept constant at 2 ml min^{-1} for 6 h to guarantee that all ethanol was completely removed. The autoclave was subsequently depressurized by 5 bar min^{-1} over 20 min before removal of the obtained aerogel. Samples were characterised immediately.

Densities of the samples were determined by weighing the aerogel monoliths on an analytical balance (0.01 mg accuracy) and measuring their dimensions using a digital calliper (±0.02 mm). Dimensions for each aerogel were taken at five different positions, and a minimum of four different aerogels were used for density determination for each nanowhisker content.

Porosity of the sample (P) was calculated using the density of the samples (d_p) and the density of the bulk cellulose nanowhiskers (d_b = 1.59 g cm^{-3}) using eqn (1), obtained from the simple mixing rule with the gas density negligible.

$$P = \left(1 - \frac{d_p}{d_b}\right) \times 100 \quad (1)$$

Powder X-ray diffraction of cellulose aerogels determined the effect of the aerogel preparation method on the crystalline structure of the cellulose nanowhiskers. Diffraction patterns of aerogels ground to a fine powder were obtained using a Phillips X'pert PW 3710 diffractometer with a Cu-Kα radiation source operating at 40 kV and 40 mA. The diffraction patterns were recorded using a step size of 0.02° between 5° and 40° angles and a scan step time of 1 s.

BET analysis of all samples was run on a Micrometrics ASAP 2000.[19] N_2 adsorption and desorption at 77 K was utilised to determine the specific surface area of the prepared aerogels.

† **Safety note**: Experiments with $scCO_2$ involve high pressures and should only be carried out in equipment with the appropriate pressure rating and safety operating procedures.

From the obtained isotherms the BET surface area and the BJH pore size distribution were calculated.[20]

Electron micrographs of aerogel samples were obtained using environmental scanning electron microscopy (ESEM) on an FEI XL30 FEG ESEM instrument operating at an acceleration voltage range of 5–10 kV. TEM micrographs of cellulose nanowhiskers were recorded on an FEI Tecnai 12 BioTwin electron microscope operating at an acceleration voltage of 80 kV. A carbon-coated Cu grid was treated under a 25% oxygen in argon plasma for 5 s. A suspension of nanoparticles was deposited on the grid and left for 3 min after which excess liquid was removed. The grid was then stained using a 2% uranyl acetate in water solution for 5 min and dried before analysis. Transmission electron micrographs of cellulose aerogels were obtained on a JEOL 2100F TEM operating at 100 kV. Small fractions were broken off of the aerogel monolith and placed in a small volume of acetone. A small droplet containing an aerogel fraction was placed on a carbon coated Cu grid and the acetone was allowed to evaporate. Micrographs could only be taken at the extremities of the fractions as middle sections were too thick to allow electron transmission.

Results and discussion

The electron micrograph of cotton nanowhiskers (Fig. 1) clearly shows their rod-like structure. The nanowhiskers tend to align in bundles along their longitudinal axis due to hydrogen bonding interactions. It is these interactions which can be used to form stable networks, even under aqueous conditions, after drying.[17]

Cellulose nanowhisker hydrogels were formed by sonication of various amounts of freeze-dried cellulose nanowhiskers in 1 ml of deionized water in a sonicating bath for 30–60 min. Sonication dispersed the nanowhiskers over the 1 ml volume allowing them to form a 3D percolated network through hydrogen bonding between surface hydroxyl groups. The required sonicating time for gelation depended on the nanowhisker content and was determined by the absence of flow upon inversion of the vial. The composition of the sonicating solutions and required sonication time is reported in Table 1. It was determined that a four day solvent exchange with ethanol, followed by 6 h $scCO_2$ (40 °C, 100 bar) drying at a flow rate of 2 ml min^{-1} resulted in completely dry aerogel monoliths. No shrinkage was noticed during solvent exchange and after $scCO_2$ drying, although this is difficult to assess accurately through visual inspection.

Fig. 2(a) shows the variation in average density of the aerogels, which ranges from 0.078 g cm^{-3} to 0.155 g cm^{-3}, as a function of cellulose nanowhisker mass. These values are consistent with densities reported for other cellulose aerogels.[14,21] The porosity

Table 1 The quantities of cellulose nanowhiskers used to produce aerogels of varying concentrations (wt%)

Cellulose nanowhiskers/mg	Deionised water/ml	Sonication time/min
80	1	60
90	1	60
100	1	60
120	1	45
140	1	45
160	1	30

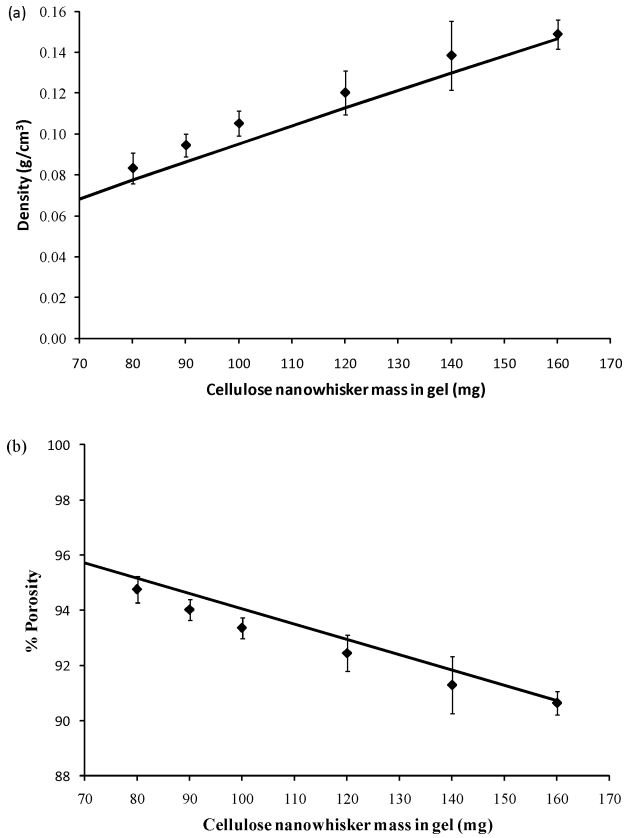

Fig. 2 (a) Aerogel density in (g cm^{-3}) and (b) porosity (%) as a function of cellulose nanowhisker content in the original hydrogel. The lines are theoretical predictions if no gel shrinkage during drying occurs.

decreases in line with the density increase (eqn (1)) from 95% to 91% (Fig. 2(b)). Assuming that the hydrogel formation occurs in the total 1 ml water volume, and that there is no shrinkage during solvent exchange and drying, it is possible to predict the theoretical density and porosity of the ideal aerogel (lines in Fig. 2(a) and (b)). One can clearly see that the experimental data match the theoretical predictions extremely well, proving the visual observation that gelation occurs over the complete water volume and that only limited shrinkage occurs during solvent exchange and drying. On average, the gels shrunk only 6.5%, in line with the lowest value in the reported range of 6.5% to 30% and even 75%.[14,22] We believe that this is due to the high modulus of the highly crystalline cellulose nanowhiskers (50–100 GPa [23]), which inhibits the sections between hydrogen bonds from collapsing.

Powder X-ray diffraction was used to probe the crystallinity of the cellulose nanowhiskers after the aerogel production. Fig. 3 compares the diffraction patterns of the aerogels with those of cellulose nanowhiskers. The diffraction pattern is consistent with the pattern for the cellulose I_β polymorph[24] as expected for cotton derived cellulose nanowhiskers with the 200 diffraction centered around 22.7°, and the double peak signal at 14.5° and 16° for $1\bar{1}0$ and 110 respectively.[25] A small peak around 20° due to 102 diffraction is also noticed. The aerogels show a clear retention of the cellulose I_β structure. Using the diffraction pattern, the relative crystallinity index was calculated to quantify the degree of crystallinity:[26]

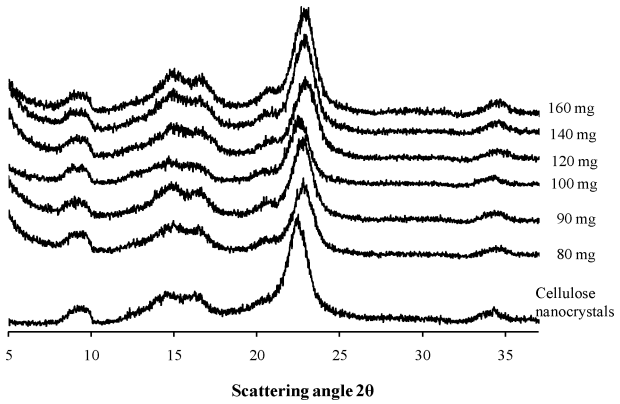

Fig. 3 XRD traces *versus* scattering angle of the cellulose nanowhiskers and cellulose nanowhisker aerogels.

$$\left(\frac{I_{22.7} - I_{18}}{I_{22.7}}\right) \times 100 \qquad (2)$$

where $I_{22.7}$ is the intensity, above the baseline, of the 020 peak maximum near to 22.7°, and I_{18} is the intensity, above the baseline, between the 020 and 110/1$\bar{1}$0 peaks, near to 18°. The relative crystallinity index is about 88.6%, in agreement with other literature values,[15] and was found to remain virtually constant for all samples. Thus, neither the sonication step or $scCO_2$ drying step affect the crystalline structure of the cellulose nanowhiskers and the aerogels are indeed porous three-dimensional structures of highly crystalline cellulose nanowhiskers.

The internal specific surface area determined through N_2 sorption experiments of the obtained aerogels was found to vary between 216 m^2 g^{-1} and 605 m^2 g^{-1}, without a clear correlation between the cellulose nanowhisker content in the original hydrogel (Fig. 4). Since the BET surface area describes the nanowhisker area which is accessible to gas adsorption, the surface area is dependent on the extent of nanowhisker indivualisation (as aggregation will reduce the accessible adsorption surface). Using the average cotton cellulose nanowhisker dimensions (6 nm × 6 nm × 180 nm) determined by Elazzouzi-Hafraoui *et al.*,[15] the specific surface area is calculated to be 419 m^2 g^{-1}, right in the middle of the experimental values. This value would be correct for an aerogel constituted of completely individualised nanowhiskers which are monodisperse and have a smooth surface. However, the dimensions of cellulose nanowhiskers are not monodisperse[15] and their surface is not smooth, both factors enabling higher specific surface areas. Lower values can be attributed to significant nanowhisker aggregation.

The nitrogen adsorption isotherms (Fig. 4 insert is representative of all aerogel isotherms) were similar to recently reported isotherms for cotton linter and bacterial cellulose aerogels.[14,22] The isotherm shape points towards a mesoporous aerogel with a significant amount of larger pores.

The total pore volume per unit volume can be calculated directly from the porosity and the aerogel density while BET measurements can be used to determine the pore volume of pores below 200 nm, as well as mesopore and micropore volume.

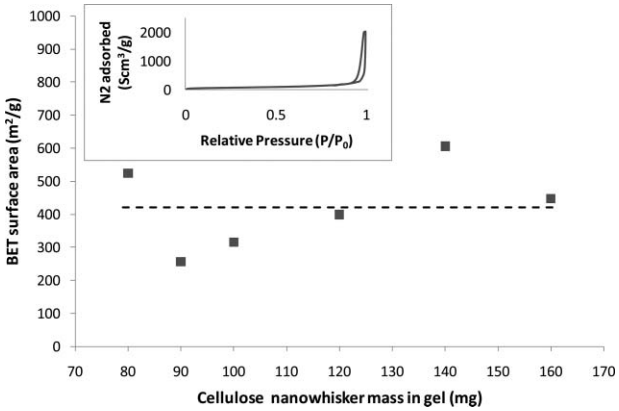

Fig. 4 BET surface area as a function of the cellulose nanowhisker content in the original hydrogel. The dotted line denotes the theoretically calculated specific surface area for the cellulose nanowhiskers using the average dimensions and assuming no polydispersity. The insert shows a typical adsorption isotherm for these aerogels.

The nitrogen adsorption isotherms can also be used to estimate the mesopore size distribution.

Micropore and mesopore volume (from N_2 adsorption measurements) and total pore volume (from mixing rule calculations using cellulose nanowhisker and aerogel density) are shown in Table 2 and Fig. 5. Microporosity (pores <2 nm) is very limited (less than 0.1–0.8%), while mesoporosity constitutes roughly 4–11% of total porosity. As the cellulose nanowhisker content increases, so does the fraction of pores which are mesopores and micropores, while the total pore volume continuously decreases. It can also be seen from comparison of Fig. 4 and 5 that the variation in mesoporosity and microporosity is consistent with the variation in measured BET surface area, as is expected. We can thus conclude that a significant amount of macropores exist in the aerogel structure. As the pore size of this fraction is largely above 200 nm (above the average length of the nanowhiskers), these pores can only form as a result of imperfect homogenisation of the nanoparticles over the hydrogel volume. As the contribution of macropores to the specific surface area is rather limited, it can be expected that better homogenisation and thus individualisation of the nanowhiskers in the hydrogel during the sonication driven gelation will lead to even higher specific surface areas.

We also determined the mesopore structure using the common BJH method.[16] A bimodal distribution is obtained with a large

Table 2 Pore volume for different pore size ranges

Cellulose nanowhisker mass in gel/mg	Micropore volume[a]/cm^3 g^{-1}	Mesopore volume[b]/cm^3 g^{-1}	Total pore volume[c]/cm^3 g^{-1}
80	0.051	0.533	11.37
90	0.012	0.366	9.94
100	0.018	0.402	8.87
120	0.039	0.438	7.69
140	0.053	0.641	6.60
160	0.019	0.621	6.09

[a] Determined from N_2 adsorption t-plot fitting. [b] Determined from N_2 adsorption measurements. [c] Calculated from sample and cellulose nanowhiskers density.

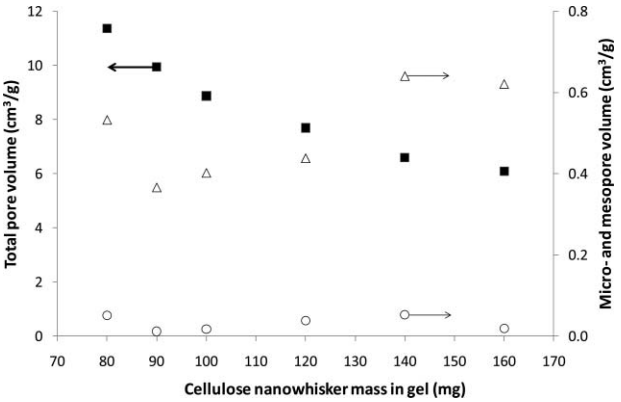

Fig. 5 Pore volume trends (■ for total pore volume, ○ for micropores, and △ for mesopores) for cellulose nanowhisker aerogels as a function of the cellulose nanowhisker mass in the original hydrogel.

maximum around 4.3 nm and a smaller peak around 15.5 nm (Fig. 6 for an 80 mg aerogel). The mesopore size distribution was found to be similar for all aerogels with the maxima for the bimodal distribution peaks stable at roughly the same positions (4.2–4.4 nm and 15.4–15.6 nm) as shown in Fig. 6 (insert). This is surprising as there is a significant variation in density and porosity as the cellulose nanowhisker content of the aerogels changes. This indicates that there exist mesoporous regions with similar characteristics in between the macropores possibly due to a specific manner in which cellulose nanowhiskers hydrogen bond into the gelled structure. The hydrogel formation kinetics and the effect of sonication on nanowhisker individualisation is currently under investigation.

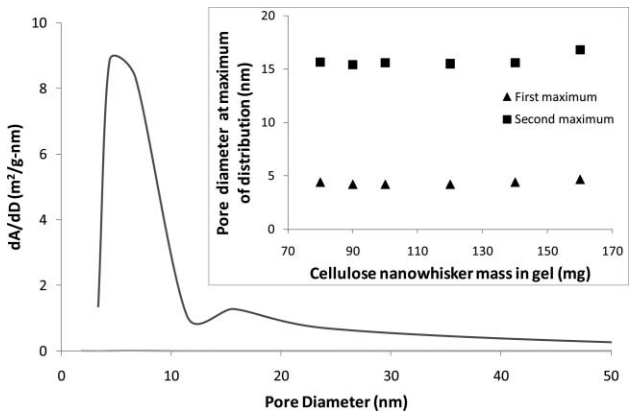

Fig. 6 Mesopore size distribution for the 80 mg cellulose nanowhisker aerogel from BJH analysis based on pore area. This distribution is representative of all the samples prepared. The insert shows the trend of the maxima of the bimodal pore size distribution of cellulose nanowhisker aerogels as a function of the cellulose nanowhisker content in the original hydrogel.

To look at the internal structure of the aerogels, the aerogel monoliths were broken in two and the surface of the fracture surface was imaged using an environmental scanning electron microscope (ESEM). Fig. 7(a) shows a representative micrograph taken of an 80 mg aerogel. A highly porous internal network is clearly visible with large pores in the sub-50 μm range. The mesoporous subsystem evidenced by N_2 adsorption measurements is not visible in the SEM image but can be seen

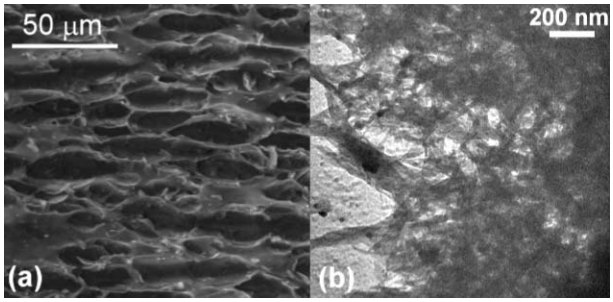

Fig. 7 (a) Scanning electron micrograph of a fractured 80 mg cellulose nanowhisker aerogel and (b) transmission electron micrograph of a section broken off from an 80 mg cellulose nanowhisker aerogel.

in the higher resolution TEM image (Fig. 7(b)). The structure is clearly highly porous with pore sizes in the nanometre range. It can be expected that the visualised sections will display pores that do not accurately show the dimensions found in the bulk of an undamaged aerogel as these sections have been broken off and have been submerged in acetone. While the latter did not break the aerogel apart without extensive mechanical agitation, it can be expected that some swelling will occur and some pore collapse may occur during drying. However, the pore structure is clearly visible in the micrograph.

Conclusions

We have successfully prepared cellulose aerogels with low densities (down to 0.078 g cm^{-3}) and some of the highest reported specific surface areas (up to 605 m^2 g^{-1}) for cellulose-based aerogels to date. These highly porous, lightweight aerogels were prepared through benign means with limited gel shrinkage during aging and drying. The density and porosity of the aerogel can be easily manipulated by varying the initial cellulose nanowhisker concentration and can be theoretically predicted. The crystalline structure of the cellulose nanowhiskers is retained throughout the aerogel production procedure, making the aerogels truly a three-dimensional assembly of cellulose nanowhiskers. The variability in specific surface area is believed to be due to variability in the hydrogel formation and we are currently investigating the ultrasound gelation kinetics and process. Aerogels kept for several weeks retained their mechanical integrity and did not show visible degradation.

It is important to note that the simplicity of the described aerogel fabrication makes these aerogels extremely versatile towards the incorporation of other nanoscale materials and this is also being pursued at current.

Acknowledgements

The authors thank the UK Engineering and Physical Sciences Research Council (EPSRC) for funding this work through the DICE (Driving Innovation in Chemistry and Chemical Engineering) Project under the Science and Innovation Award (Grant Number EP/D501229/1). They also thank Prof. Robert Mokaya for the use of his gas adsorption equipment and Dr Mike Fay for his help with electron microscopy.

Notes and references

1 E. Guilminot, F. Fischer, M. Chatenet, A. Rigacci, S. Berthon-Fabry, P. Achard and E. Chainet, *J. Power Sources*, 2007, **166**, 104.
2 S. S. Kistler, *Nature*, 1931, **127**, 741; S. S. Kistler, *J. Phys. Chem.*, 1932, **36**, 52.
3 J. Cai, S. Kimura, M. Wada, S. Kuga and L. Zhang, *ChemSusChem*, 2008, **1**, 149.
4 M. Mukhopadhyay and B. S. Rao, *J. Chem. Technol. Biotechnol.*, 2008, **83**, 1101.
5 J. Choi and D. J. Suh, *Catal. Surv. Asia*, 2007, **11**, 123.
6 N. Hüsing and U. Schubert, *Angew. Chem., Int. Ed.*, 1998, **37**, 22.
7 C. Tsioptsias, A. Stefopoulos, I. Kokkinomalis, L. Papadopoulou and C. Panayiotou, *Green Chem.*, 2008, **10**, 965.
8 O. Aaltonen and O. Jauhiainen, *Carbohydr. Polym.*, 2009, **75**, 125.
9 R. Gavillon and T. Budtova, *Biomacromolecules*, 2008, **9**, 269.
10 S. Hoepfner, L. Ratke and B. Milow, *Cellulose*, 2008, **15**, 121; F. Fischer, A. Rigacci, R. Pirard, S. Berthon-Fabry and P. Achard, *Polymer*, 2006, **47**, 7636; H. Jin, Y. Nishiyama, M. Wada and S. Kuga, *Colloids Surf., A*, 2004, **240**, 63; C. Tan, B. M. Fung, J. K. Newman and C. Vu, *Adv. Mater.*, 2001, **13**, 644.
11 M. Pääkko, J. Vapaavuori, R. Silvennoinen, M. Ankerfors, T. Lindström, L. A. Berglund and O. Ikkala, *Soft Matter*, 2008, **4**, 2492.
12 M. D. Gawryla, O. Van Den Berg, C. Weder and D. A. Schiraldi, *J. Mater. Chem.*, 2009, **19**, 2118.
13 W. Thielemans, M. N. Belgacem and A. Dufresne, *Langmuir*, 2006, **22**, 4804.
14 F. Liebner, E. Haimer, M. Wendland, M.-A. Neouze, K. Schlufter, P. Miethe, T. Heinze, A. Potthast and T. Rosenau, *Macromol. Biosci.*, 2010, **10**, 349.
15 S. Elazzouzi-Hafraoui, Y. Nishiyama, J.-L. Putaux, L. Heux, F. Dubreuil and C. Rochas, *Biomacromolecules*, 2008, **9**, 57.
16 S. J. Eichhorn, A. Dufresne, M. Aranguren, N. E. Marcovich, J. R. Capadona, S. J. Rowan, C. Weder, W. Thielemans, M. Toman, S. Renneckar, W. Gindl, S. Veigel, J. Keckes, H. Yano, K. Abe, M. Nogi, A. N. Nakagaito, A. Mangalam, J. Simonsen, A. S. Benight, A. Bismarck, L. A. Berglund and T. Peijs, *J. Mater. Sci.*, 2010, **45**, 1.
17 M. J. Bonné, K. Edler, J. G. Buchanan, D. Wolverson, E. Psillakis, M. Helton, W. Thielemans and F. Marken, *J. Phys. Chem. C*, 2008, **112**, 2660; W. Thielemans, C. R. Warbey and D. A. Walsh, *Green Chem.*, 2009, **11**, 531.
18 P. C. S. Tischer, M. R. Sierakowski, H. Westfahl, Jr. and C. A. Tischer, *Biomacromolecules*, 2010, **11**, 1217.
19 S. Brunauer, P. H. Emmett and E. Teller, *J. Am. Chem. Soc.*, 1938, **60**, 309.
20 E. P. Barrett, L. G. Joyner and P. P. Halenda, *J. Am. Chem. Soc.*, 1951, **73**, 373.
21 J. Innerlohinger, H. K. Weber and G. Kraft, *Macromol. Symp.*, 2006, **244**, 126.
22 F. Liebner, E. Haimer, A. Potthast, D. Loidl, S. Tschegg, M.-A. Neouze, M. Wendland and T. Rosenau, *Holzforschung*, 2009, **63**, 3.
23 R. Rusli and S. J. Eichhorn, *Appl. Phys. Lett.*, 2008, **93**, 033111.
24 Y. Nishiyama, P. Langan and H. Chanzy, *J. Am. Chem. Soc.*, 2002, **124**, 9074.
25 G. Morandi, L. Heath and W. Thielemans, *Langmuir*, 2009, **25**, 8280.
26 P. J. Weimer, J. M. Hackney and A. D. French, *Biotechnol. Bioeng.*, 1995, **48**, 169.